2019

Do genetic structure and landscape heterogeneity impact color morph frequency in a polymorphic salamander?

Maggie M. Hantak
Ohio Center for Ecological and Evolutionary Studies

Robert B. Page
Texas A&M University

Paul E. Converse
Ohio Center for Ecological and Evolutionary Studies

Carl D. Anthony
John Carroll University, canthony@jcu.edu

Shawn R. Kuchta
Ohio Center for ecological and Evolutionary Studies

Research

Do genetic structure and landscape heterogeneity impact color morph frequency in a polymorphic salamander?

Maggie M. Hantak, Robert B. Page, Paul E. Converse, Carl D. Anthony, Cari-Ann M. Hickerson and Shawn R. Kuchta

Landscape heterogeneity plays an important role in population structure and divergence, particularly for species with limited vagility. Here, we used a landscape genetic approach to identify how landscape and environmental variables affect genetic structure and color morph frequency in a polymorphic salamander. The eastern red-backed salamander, *Plethodon cinereus*, is widely distributed in northeastern North America and contains two common color morphs, striped and unstriped, that are divergent in ecology, behavior, and physiology. To quantify population structure, rates of gene flow, and genetic drift, we amplified 10 microsatellite loci from 648 individuals across 28 sampling localities. This study was conducted in northern Ohio, where populations of *P. cinereus* exhibit an unusually wide range of morph frequency variation. To test whether genetic distance was more correlated with morph frequency, elevation, canopy cover, waterways, ecological niche or geographic distance, we used resistance distance and least cost path analyses. We then examined whether landscape and environmental variables, genetic distance or geographic distance were correlated with variation in morph frequency. Tests for population structure revealed three genetic clusters across our sampling range, with one cluster monomorphic for the striped morph. Rates of gene flow and genetic drift were low to moderate across sites. Genetic distance was most correlated with ecological niche, elevation and a combination of landscape and environmental variables. In contrast, morph frequency variation was correlated with waterways and geographic distance. Thus, our results suggest that selection is also an important evolutionary force across our sites, and a balance between gene flow, genetic drift and selection interact to maintain the two color morphs.

Keywords: ecological niche model, gene flow, genetic drift, microsatellite, Plethodontidae

Introduction

Landscape genetics combines landscape ecology, population genetics, and spatial statistics to quantify the relative contribution of environmental and landscape features on patterns of genetic connectivity (Manel et al. 2003, Manel and Holderegger 2013).

Heterogeneity across a landscape can greatly impact population connectivity, particularly for dispersal-limited species (Spear et al. 2005, Wang 2009, Peterman and Semlitsch 2013). Population genetic structure may vary as a consequence of environmental preferences, mate selection, species interactions or the demographic history of populations (Slatkin 1987, Storfer et al. 2007). In addition, phenotypic divergence can influence genetic structure and gene flow, which may result in reproductive isolation and speciation (Wang and Summers 2010); however, the ubiquity of this relationship is unknown.

Color polymorphic species, where two or more discrete color morphs coexist within a population, represent an ideal system to investigate the ecological and evolutionary processes that contribute to population divergence (Ford 1945). Although color polymorphism is a classic subject in evolutionary biology (Cain and Sheppard 1954, Endler 1978), little attention has been given to the geographic context of polymorphisms, with most studies focusing on in-depth investigations of single populations (Sinervo and Lively 1996, Svensson et al. 2001, Hantak et al. 2016; but see Corl et al. 2010, Davis Rabosky et al. 2016 for notable exceptions). Morphs represent contrasting character sets that are the consequence of multivariate disruptive natural selection acting on the same genome (Sinervo and Svensson 2002), and are important, in part because they allow a single species to occupy multiple niches within a single population (West-Eberhard 1986, Forsman et al. 2008). Evolutionary processes that operate to maintain polymorphisms include overdominance, negative frequency-dependent selection, spatiotemporal variation in selection, and gene flow among populations (Allen 1988, Gray and McKinnon 2007). Gene flow is noteworthy because it can maintain a polymorphism despite diversifying selection among populations (Slatkin 1987, Sandoval 1994). In contrast, when gene flow is low, geographic distance, genetic drift, natural selection or a combination of these mechanisms can promote morph frequency divergence (including fixation) among populations (Sandoval 1994).

Here we examine how genetic differentiation, landscape features, gene flow and genetic drift impact color morph frequency among populations of the polymorphic eastern red-backed salamander, *Plethodon cinereus*. Within the salamander family Plethodontidae, the genus *Plethodon* contains 10 species that display a striped/unstriped color polymorphism (Highton 2004). The 'striped' morph possesses a red stripe overlaid on a black dorsum, whereas the 'unstriped' morph has a completely black dorsum (Highton 1962; Fig. 1a). The color morphs are divergent along multiple niche axes, including dietary composition, temperature associations, metabolic rate, territorial behavior and mating interactions (summarized in Anthony and Pfingsten 2013; see also Acord et al. 2013, Reiter et al. 2014, Paluh et al. 2015, Stuczka et al. 2016). It is likely that correlational selection has acted on suites of traits to produce the covariant, differentially adapted character sets that define the morphs (Sinervo and Svensson 2002). *Plethodon cinereus* provides an ideal opportunity for studying polymorphism in a geographic framework as both morphs are common, population sizes are large, and dispersal is limited (Burton and Likens 1975, Liebgold et al. 2011).

Our study is focused on a set of populations in postglacial, northern Ohio that display unusually high variation in morph frequency, including populations that are monomorphic for both morphs (Fig. 1a). Using microsatellite loci, we quantified genetic structure among our sampled populations. Then, we tested whether morph frequency, geographic distance, or landscape variables better explain patterns of genetic variation in *P. cinereus*. The usual expectation, and our null hypothesis, is isolation by distance; however, genetic differentiation in amphibians is often associated more strongly with phenotypic variation than with geography (Funk et al. 2009, Wang and Summers 2010). Geographic distance, genetic variation and landscape variables can also directly influence geographic variation in polymorphisms (McLean et al. 2015); thus, we examined the contribution of these factors in influencing patterns of morph frequency variation in *P. cinereus*. Lastly, we tested whether gene flow and/or genetic drift impact the distribution of color morphs in northern Ohio. As morphs of *P. cinereus* compete over resources (Anthony et al. 2008, 2017), morphs may be adapted to their local environments, rendering populations differing in morph frequencies divergent in ecology and behavior. Accordingly, we hypothesized reduced gene flow between populations that are more divergent in morph frequency.

Methods

Population sampling and laboratory techniques

We collected tissue from small salamander tail tips (Cabe et al. 2007) from 648 individuals of *Plethodon cinereus* from 28 populations in northern Ohio between spring 2015 and fall 2016 (Fig. 1a). Tissue samples were immediately preserved in 95% ethanol. Genomic DNA was extracted using Qiagen DNeasy tissue kits following the manufacturer's protocol. We amplified 10 microsatellite loci, with tri-pentanucleotide repeat motifs, developed for *P. cinereus* (Pc3, Pc7, Pc15–Pc17, Pc25, Pc28, Pc30, Pc34, Pc37; Cameron et al. 2017) using PCR. Forward primers were modified with a 5′ florescent tag of 6-FAM, NED, HEX, PET or ATTO 565 (NHS Ester), and were multiplexed in an arrangement of 3–4 loci. PCR products were run on an ABI 3730 DNA Analyzer using a LIZ 600 size standard at the Arizona State University CLAS DNA Laboratory. Scoring and binning were done in Geneious ver. 9.1.8 (Kearse et al. 2012).

Population genetic analyses

We used MICRO-CHECKER ver. 2.2 (van Oosterhout et al. 2004) to check for scoring errors and used 10 000 Monte

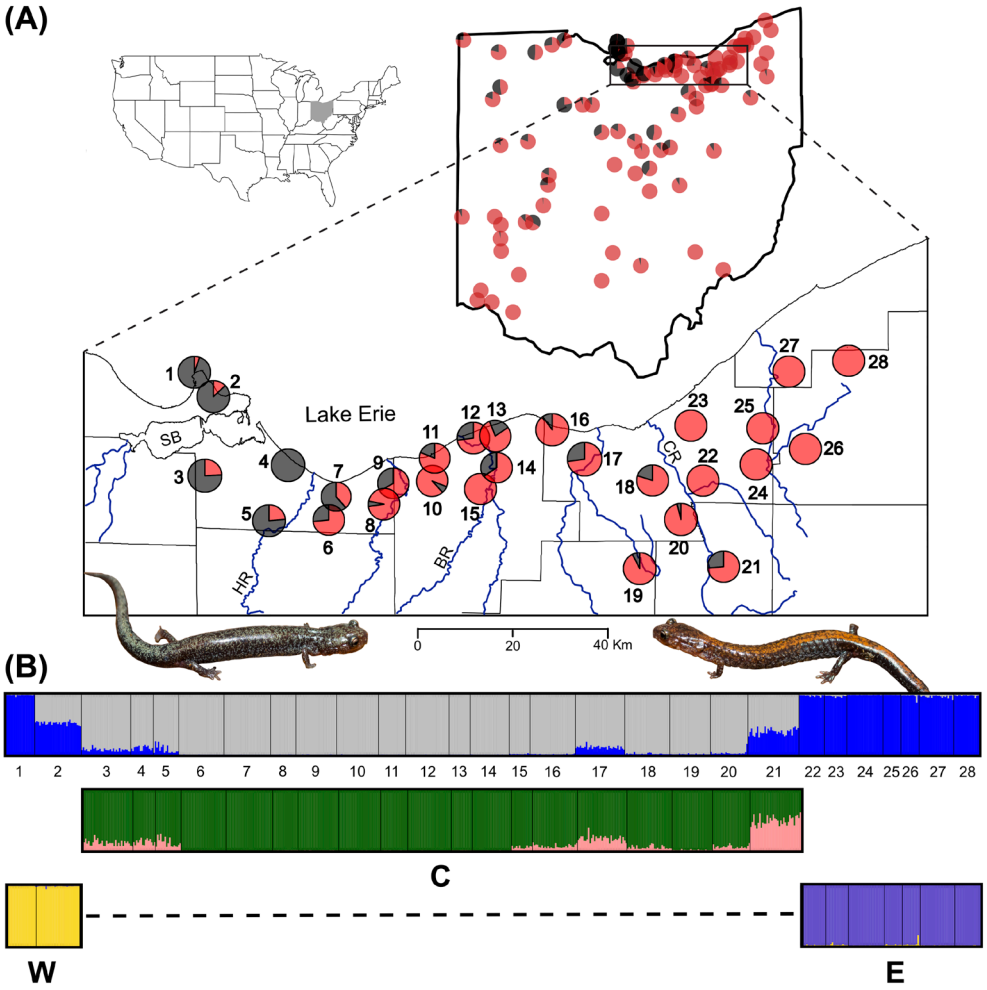

Figure 1. (A) Sampling localities with morph frequencies (gray = unstriped, red = striped morph) throughout Ohio. Important waterways are denoted: Cuyahoga River (CR), Black River (BR), Huron River (HR) and Sandusky Bay (SB). The unstriped morph is depicted in the bottom left and the striped morph in the bottom right. (B) STRUCTURE results for all populations, and clusters found by looking at substructure: C = 'Central Cluster', W = 'Western Cluster' and E = 'Eastern Cluster'. Sampling localities match A.

Carlo simulations to test for the presence of null alleles. The R package genepop (Rousset et al. 2008) was used to test for linkage disequilibrium among pairs of loci and to identify whether loci within populations conformed to Hardy–Weinberg equilibrium (HWE). Allele number (N_A), observed heterozygosity (H_O), and expected heterozygosity (H_E) were calculated in GENALEX ver. 6.5 (Peakall and Smouse 2012). Rarefied allelic richness (A_R) and rarefied private allelic richness (pA_R) were calculated in HP-RARE (Kalinowski 2005). We used GENODIVE ver. 2.0 (Meirmans and van Tienderen 2004) to calculate pairwise F_{ST}, standardized F_{ST} (F'_{ST}) and Jost's D values (D_{est}; Jost 2008) between localities.

We used STRUCTURE ver. 2.3 (Pritchard et al. 2000) to identify genotypic clusters from sampled localities. Structure was run from K = 1 to K = 28 populations, with a burn-in of 250 000 and 600 000 Markov chain Monte Carlo (MCMC) iterations after burn-in. Each K was replicated 10 times with random starting seeds. We used STRUCTURE HARVESTER ver. 0.6.94 (Earl and vonHoldt 2012) to obtain ΔK using the Evanno method, which is based on the rate of change in the log probability of data between successive K-values (Evanno et al. 2005, Janes et al. 2017). To find optimal alignments from the 10 iterations for each cluster we used the program CLUMPP ver. 1.1 (Jakobsson and Rosenberg 2007). Results from STRUCTURE and CLUMPP were visualized using DISTRUCT ver. 1.1 (Rosenberg 2004). As the Evanno method recovers the basal level of genetic structure, this procedure was replicated iteratively within clusters to detect substructure (Janes et al. 2017). We also used a discriminant analysis of principal components (DAPC) to test for population structure using the R package adegenet (Jombart 2008). In contrast with STRUCTURE, DAPC investigates patterns of population differentiation without assuming a model of evolution (Jombart et al. 2010). We explored a range of K-values using K-means clustering and Bayesian information criteria (BIC). Cross-validation was used to determine the number of PC axes to retain (Jombart et al. 2010).

Gene flow and genetic drift

Gene flow was estimated using MIGRATE-N ver. 3.6.11 in the CIPRES Science Gateway ver. .3.3 (Beerli 2008, Beerli and Palczewski 2010). MIGRATE-N uses a coalescent framework to estimate gene flow across populations. We used a Brownian motion model with three independent runs and three replicates within each run. Runs consisted of one long chain of 10 000 generations sampled every 500 increments, with 5000 iterations excluded as burn-in. Four parallel, heated chains were used with temperatures of 1.0, 1.5, 3.0 and 1 000 000. Our large number of populations and individuals exceeded the computational limits of MIGRATE-N. Therefore, we ran MIGRATE-N within one genetic cluster that was comprised of 19 populations that were highly variable in morph frequency; to improve speed we grouped geographically close populations with similar morph frequencies (3+5, 6+7, 10+11, 12+13, 17+18, 19+20). Most combined sites were <10% divergent in morph frequency; the exception are sites 6+7, which differed by 30%, but we grouped these two populations because they are separated by only 3 km and had $F_{ST} = 0.02$. Population 21 was not included due to its high degree of admixture (Fig. 1b). We considered parameter estimates to be accurate if effective sample sizes were >1000 (Converse et al. 2015).

To estimate the effect of genetic drift, we used the R package RAFM to obtain Bayesian estimates of the admixture F model (AFM; Karhunen and Ovaskainen 2012). This approach assumes each of n contemporary local populations is derived from one or more evolutionarily independent lineages with a common ancestor T generations ago. RAFM estimates one vector of parameters (alpha) and two matrices of parameters (kappa and theta): alpha describes the amount of drift experienced by each of the n evolutionary lineages; kappa describes the proportional contribution of each respective lineage to each respective contemporary local population (i.e. a matrix of admixture coefficients); and theta is a pair-wise matrix of population-level coancestry coefficients. We ran RAFM with 100 000 MCMC iterations, sampled every tenth iteration, and excluded 50 000 generations as burn-in across all populations and within each cluster. We used median values across MCMC samples as best estimates of the elements within alpha and theta, and means as our best estimate for the elements of kappa.

Landscape resistance surfaces and analyses

To model dispersal in *P. cinereus*, we created landscape resistance surfaces based on features that are known to impact amphibian movement (Storfer et al. 2010). Digital elevation (DEM; 9.1×9.1 m resolution) and tree canopy coverage (30×30 m) were obtained from the U.S. Geological Survey National Map (USGS, <https://viewer.nationalmap.gov>). Rivers, streams (30×30 m) and Lake Erie (9.1×9.1 m) were created in ARCGIS ver. 10.4.1. We classified rivers, streams, and Lake Erie as binary (presence/absence) surfaces and merged raster files to create a comprehensive 'waterway' surface. Environmental variables were used to create an ecological niche model (ENM) for *P. cinereus*. Occurrence localities (n = 795) for the ENM were obtained from online biodiversity databases (GBIF, iNaturalist, iDigBio, VertNet) and our sampling sites. Our ENM was built with the maximum entropy algorithm MAXENT ver. 3.4.1 (Phillips et al. 2006) using five uncorrelated ($R \leq 0.70$) BIOCLIM variables (Supplementary material Appendix 1 Table A1) at 30 arc-second (~1 km) resolution (<www.worldclim.org>; Hijmans et al. 2005).

To quantify the relationship between genetic distance and morph frequency with landscape resistance, we employed the R package ResistanceGA (Peterman 2018). ResistanceGA uses a genetic algorithm to optimize resistance surfaces, using either a series of transformations on continuous surfaces, or a classification of resistance values on categorical surfaces (Scrucca 2013). In addition, ResistanceGA allows for resistance surface summation to create a 'composite' resistance surface, which we created from our ENM, DEM, waterways, and canopy surfaces. Prior to running ResistanceGA, each resistance surface was re-sampled at 300 m resolution due to computational limitations resulting from our large number of populations and broad sampling extent (Peterman, pers. comm.; Fig. 2). Effective resistance between the 28 sampling localities, as well as within each genetic cluster, was measured using least cost path (LCP) distance and resistance distance (RD), as implemented in the 'commuteDistance' function within the R package gdistance (van Etten 2017). LCP estimates the optimal route between two sites that minimizes the cost of moving through the landscape, whereas RD (circuit theory) assesses all possible pathways between two localities and generates a cumulative cost (Adriaensen et al. 2003, McRae 2006). All optimization runs were conducted twice (Peterman 2018).

We calculated Euclidean distances between localities to generate a geographic distance matrix, and used the equation from McLean et al. (2015) to create a morph frequency distance matrix. To determine which resistance or distance matrix was most closely correlated with genetic distance and morph frequency, we fit linear mixed models with maximum-likelihood population effects (MLPE) using the R package lme4 (Clarke et al. 2002, van Strien et al. 2012). Models were run separately for LCP and RD across all populations and within clusters. In the first set of models, linearized F_{ST} was the dependent variable, and scaled and centered effective resistance from each surface, morph frequency, and geographic distance were independent variables. To determine the factors directly affecting morph frequency variation, we created a second set of models where morph frequency was the dependent variable, and linearized F_{ST}, the scaled and centered effective resistance of each surface, and geographic distance were independent variables. We used simple,

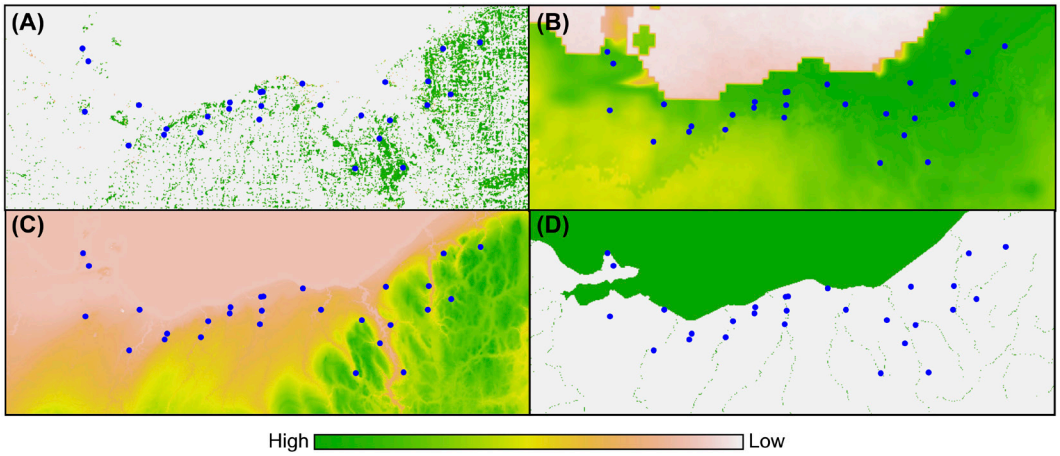

Figure 2. Landscape surfaces with sampling localities (blue circles) used in ResistanceGA. (A) Percent tree canopy, (B) Ecological niche model (ENM), (C) Digital elevation model (DEM), (D) waterways. Green represents high, yellow intermediate and white low values for each surface.

single predictor models due to a high degree of multicollinearity among surfaces (Peterman 2018). Best-fit models were assessed and ranked using AICc with the R package AICcmodavg (Mazerolle 2013).

Data deposition

Data available from the Dryad Digital Repository: <http://dx.doi.org/10.5061/dryad.j807218> (Hantak et al. 2019).

Results

Population genetic analyses

Across the 28 populations, all microsatellite loci were polymorphic, with 2–18 alleles per locus (mean = 4 ± 0.82 SD). Observed heterozygosity ranged from 0.23 to 0.58 (mean = 0.387 ± 0.10) among populations (Supplementary material Appendix 1 Table A2). Departures from HWE were found at four loci in eight sites after Bonferroni correction. MICRO-CHECKER did not indicate scoring errors, but null alleles were found at three loci in eight populations, except for Pc25, in which null alleles were found in 13 populations. No pairwise loci were in linkage disequilibrium across any populations. We retained all loci for further analyses because null alleles can have weak effects on genetic structure (Chapuis and Estoup 2007), deviations from HWE were not consistent across populations, and their elimination did not alter our results (not shown).

Genetic structure

STRUCTURE revealed a peak at ΔK = 2 (Fig. 1b, Supplementary material Appendix 1 Fig. A1). One cluster included sites from the center of the sampling range (3–21); we call this the 'Central Cluster'. Genetic admixture in the Central Cluster was low, except for site 21, and no substructure was detected within this cluster, including after removing site 21 (Supplementary material Appendix 1 Fig. A2). Further tests of substructure with the inclusion of site 2 in the Central Cluster revealed no admixture (Supplementary material Appendix 1 Fig. A3). Morph frequencies vary greatly within the Central Cluster, ranging from 100% striped to 100% unstriped (Fig. 1). The second cluster combined localities from the western and eastern ends of our sampling. Tests of substructure recovered the eastern and western regions as distinct, with no evidence of admixture. We call these the 'Western Cluster' (sites 1–2) and the 'Eastern Cluster' (sites 22–28; Fig. 1b). Western Cluster sites are nearly monomorphic for the unstriped morph (≥90%); whereas the Eastern Cluster is entirely fixed for the striped morph (Fig. 1). Using BIC, 5–10 clusters were recovered using DAPC (Supplementary material Appendix 1 Fig. A4). We chose K = 5 because it creates the most inclusive groups. The cross-validation test indicated that 15 principal components should be retained and we elected to include all discriminant functions. DAPC results were similar to the STRUCTURE results: cluster 1 = Western Cluster; clusters 2, 3, 5 (which widely overlap) = Central Cluster, plus one individual from site 2; cluster 4 = Eastern Cluster, plus 13 individuals from site 21 and 1 individual each from sites 2 and 17. Thus, the STRUCTURE and DAPC results largely correspond in recognizing three genetic clusters (Supplementary material Appendix 1 Fig. A4), with the exception of ambiguities stemming from population 21.

Genetic differentiation varied substantially among populations. F_{ST} ranged from 0 to 0.616, F'_{ST} 0–0.835, and D_{est} 0–0.753 (Supplementary material Appendix 1 Table A3, A4). In general, variation was low within clusters (Fig. 3). In the Eastern Cluster, the furthest separated sites had $F_{ST} = 0.007$ (sites 22 and 28; 41.2 km). In the Central Cluster, the furthest separated sites had $F_{ST} = 0.104$ (sites 3 and 21; 109.8 km). The

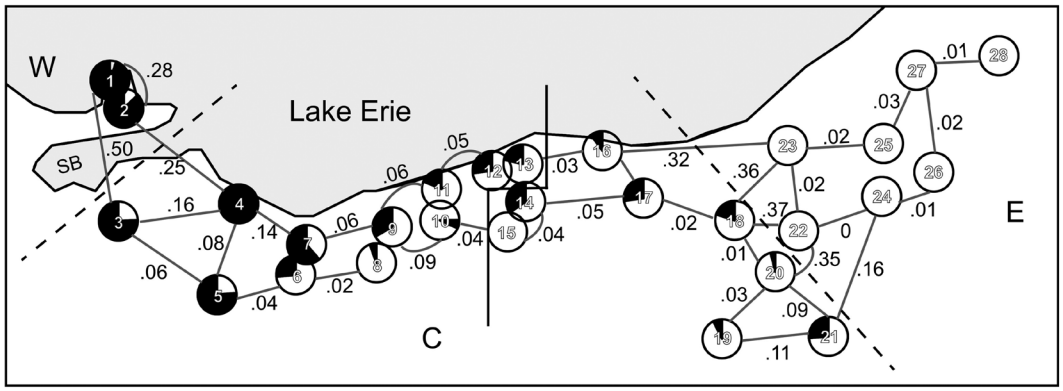

Figure 3. Map of northern Ohio sampling localities (black = unstriped, white = striped morph) with F_{ST} values between pairs of sites. Population numbers are in the center of each pie and correspond with Fig. 1. The dashed, black lines denote breaks between the three microsatellite clusters: W = 'Western Cluster', C = 'Central Cluster' and E = 'Eastern Cluster'. The solid, black line separates mtDNA clades (Radomski 2017).

two Western Cluster localities had $F_{ST} = 0.28$ (5.3 km), which is the highest intra-cluster comparison. Contrasts between clusters were high relative to intra-cluster comparisons (Fig. 3). For example, site 20 (Central Cluster) and site 22 (Eastern Cluster), which are 7.1 km apart, had $F_{ST} = 0.349$. Similarly, site 2 (Western Cluster) and site 3 (Central Cluster), which are 17.2 km apart (including Sandusky Bay), had $F_{ST} = 0.229$. Site 1 in the Western Cluster and site 3 in the Central Cluster had $F_{ST} = 0.500$ and are separated by 21.1 km, though this includes Sandusky Bay and West Harbor.

Gene flow and genetic drift

Locus Pc16 was excluded in gene flow analyses because it led to greatly reduced ESS values. In total, we recovered estimates with high consistency among three runs for 61 pairs of populations within the Central Cluster (Supplementary material Appendix 1 Table A5). Gene flow rates are presented as the proportion of migrants (m_b) between populations. Rates of gene flow were lowest between site 8 and 10 + 11 ($m = 0.007$), and between site 3 + 5 and 4 ($m = 0.007$). Gene flow was highest between site 17 + 18 and 19 + 20 ($m = 0.115$; Supplementary material Appendix 1 Fig. A5, Table A5).

Across all populations, RAFM revealed that low levels of coancestry between populations contributed to separate clusters, with increased genetic drift in lineages contributing to the Eastern and Western Clusters (Supplementary material Appendix 1 Fig. A6). Within the Western Cluster, AFM found relatively strong genetic drift with little admixture between lineages (Supplementary material Appendix 1 Fig. A7). Within the Central and Eastern Clusters, our sample sites exhibited relatively homogenous levels of coancestry; the degree of admixture varied among sites, with most sites having an admixture coefficient ≥0.50 for a particular lineage (Supplementary material Appendix 1 Fig. A8, A9). Overall, the AFM suggests that restriction of gene flow from the Central Cluster and relatively strong genetic drift within the Eastern Cluster influenced differentiation between these groups.

Factors correlated with genetic variation

Across all sites, model selection using genetic distance as a response variable differed between RD and LCP. Under RD, ENM was the best-supported predictor variable, separated from other variables by ΔAICc = 34.8 (Table 1a). In the LCP analysis, the composite surface was best-supported and separated from the second ranked predictor (ENM) by ΔAICc = 66.7 (Table 2a). Within the Central Cluster, RD and LCP recovered DEM as the highest-ranking predictor, followed by canopy cover (ΔAICc = 14.6; RD; Table 1b) and

Table 1. Resistance distance model selection from MLPE analysis with genetic distance as the dependent variable for (A) all sampling sites, (B) Central Cluster, (C) Eastern Cluster.

Surface	AIC_C	ΔAIC_C	$AIC_C Wt$	R^2_m	R^2_c
(A) All sites					
ENM	−497.45	0	1	0.51	0.71
Canopy cover	−462.62	34.84	0	0.25	0.41
Waterways	−460.29	37.17	0	0.25	0.39
Geographic distance	−456.17	41.28	0	0.21	0.39
Composite	−454.75	42.7	0	0.22	0.45
DEM	−452.34	45.11	0	0.20	0.40
Morph frequency	−384.75	112.7	0	0.06	0.28
(B) Central Cluster					
DEM	−807.44	0	1	0.53	0.78
Canopy cover	−792.81	14.63	0	0.30	0.76
Waterways	−789.39	18.05	0	0.03	0.69
ENM	−789.26	18.18	0	0.03	0.69
Composite	−788.37	19.07	0	0.03	0.69
Morph frequency	−787.08	20.36	0	0.03	0.67
Geographic distance	−785.56	21.88	0	0.02	0.68
(C) Eastern Cluster					
Composite	−116.39	0	0.74	0.68	0.68
ENM	−114.25	2.14	0.26	0.65	0.65
Canopy cover	−102.03	14.35	0	0.32	0.56
DEM	−99.06	17.33	0	0.12	0.53
Waterways	−98.29	18.09	0	0.07	0.54
Geographic distance	−97.87	18.52	0	0.04	0.51

R^2_m = marginal R^2-value; R^2_c = conditional R^2-value.

Table 2. LCP model selection from MLPE analysis with genetic distance as the dependent variable for (A) all sampling sites, (B) Central Cluster, (C) Eastern Cluster.

Surface	AIC_C	ΔAIC_C	$AIC_C Wt$	R^2_m	R^2_c
(A) All sites					
Composite	−608.79	0	1	0.62	0.71
ENM	−542.08	66.71	0	0.49	0.67
DEM	−471.53	137.26	0	0.27	0.43
Canopy cover	−471.49	137.3	0	0.26	0.40
Waterways	−457.79	151	0	0.21	0.40
Geographic distance	−456.17	152.62	0	0.21	0.39
Morph frequency	−384.75	224.04	0	0.06	0.28
(B) Central Cluster					
DEM	−821.77	0	1	0.50	0.76
ENM	−790.05	31.72	0	0.12	0.77
Canopy cover	−789.3	32.48	0	0.24	0.73
Morph frequency	−787.08	34.69	0	0.03	0.67
Composite	−786.34	35.43	0	0.02	0.68
Waterways	−785.66	36.11	0	0.02	0.68
Geographic distance	−785.56	36.21	0	0.02	0.68
(C) Eastern Cluster					
Composite	−112.81	0	0.52	0.63	0.63
ENM	−112.64	0.17	0.48	0.62	0.62
DEM	−100.43	12.38	0	0.21	0.59
Canopy cover	−99.54	13.27	0	0.19	0.51
Waterways	−98.08	14.73	0	0.05	0.51
Geographic distance	−97.87	14.94	0	0.04	0.51

R^2_m = marginal R^2-value; R^2_c = conditional R^2-value.

ENM (ΔAICc = 31.7; LCP; Table 2b). Within the Eastern Cluster, RD and LCP identified the composite surface as best-supported, however, ENM was also well supported (RD ΔAICc = 2.1, Table 1c; LCP ΔAICc = 0.2, Table 2c).

Factors correlated with morph frequency variation

Predictors of morph frequency variation were discordant between RD and LCP models. Under RD, waterways were the best-supported predictor variable across all populations and within the Central Cluster (Table 3a–b). Across all populations, DEM ranked second (ΔAICc = 12.98), and within the Central Cluster geographic distance ranked second (ΔAICc = 5.4; Table 3a–b). In the LCP analysis, across all populations and within the Central Cluster, geographic distance was top-ranked (Table 3c–d), followed by canopy cover across all populations (ΔAICc = 5.47). Within the Central Cluster, waterways were the second most important predictor variable (ΔAICc = 0.16; Table 3c–d).

Discussion

In this paper, we examined and compared factors that correlate with geographic variation in the striped/unstriped polymorphism in *Plethodon cinereus*. Across 28 sampling localities in northern Ohio, we found evidence for three genetic clusters (Western, Central and Eastern; Fig. 1). The Western Cluster includes two sites (1–2), both of which have a high frequency

Table 3. Results of MLPE analysis with morph frequency as the dependent variable for resistance distance (RD) model selection across (A) all sampling sites, (B) Central Cluster; LCP model selection across (C) all sampling sites, (D) Central Cluster.

Surface	AIC_C	ΔAIC_C	$AIC_C Wt$	R^2_m	R^2_c
(A) RD All sites					
Waterways	92.23	0	1	0.41	0.57
DEM	105.21	12.98	0	0.36	0.52
Geographic distance	109.88	17.65	0	0.33	0.55
Canopy cover	125.57	33.35	0	0.33	0.57
Composite	159.08	66.85	0	0.25	0.57
ENM	213.1	120.87	0	0.29	0.70
F_{ST}	260.28	168.05	0	0.05	0.33
(B) RD Central Cluster					
Waterways	27.55	0	0.85	0.20	0.52
Geographic distance	32.89	5.35	0.06	0.16	0.51
ENM	32.92	5.38	0.06	0.19	0.49
DEM	34.01	6.47	0.03	0.50	0.69
Composite	38.32	10.77	0	0.16	0.48
F_{ST}	53.12	25.57	0	0.15	0.42
Canopy cover	55.92	28.38	0	0.25	0.63
(C) LCP All sites					
Geographic distance	109.88	0	0.94	0.33	0.55
Canopy cover	115.34	5.47	0.06	0.34	0.55
DEM	124.14	14.26	0	0.32	0.58
Waterways	124.3	14.42	0	0.30	0.54
Composite	209.48	99.6	0	0.24	0.53
ENM	229.06	119.18	0	0.17	0.54
F_{ST}	260.28	150.4	0	0.05	0.33
(D) LCP Central Custer					
Geographic distance	32.89	0	0.4	0.16	0.51
Waterways	33.05	0.16	0.37	0.16	0.51
DEM	35.39	2.5	0.12	0.39	0.58
Composite	35.47	2.58	0.11	0.14	0.51
F_{ST}	53.12	20.23	0	0.15	0.42
Canopy cover	54.32	21.43	0	0.32	0.72
ENM	63.52	30.63	0	0.01	0.45

R^2_m = marginal R^2-value; R^2_c = conditional R^2-value.

of the unstriped morph (≥90%; Fig. 1a), a situation that is uncommon across the range of *P. cinereus* (Cosentino et al. 2017). The Central Cluster includes localities 3–21 and exhibits a high variation in morph frequency among populations. The Eastern Cluster includes sites 22–28, all of which are fixed for the striped morph.

Across all populations, genetic distance was most correlated with our ENM using RD. In contrast, LCP genetic distance was correlated with a combination of ecological and landscape features (our 'composite model'). Other studies have also documented discrepancies between RD and LCP as measures of effective resistance (Avon and Bergès 2016, McClure et al. 2016). In general, RD is more sensitive to raster surface aggregation, whereas LCP is more sensitive to the number of pixels representing a landscape and the Euclidean distance between populations (Marrotte and Bowman 2017). In our study, model discordance may be related to the computational complexity that results from combining genetic clusters. In the Central Cluster, RD and LCP were best fit by the DEM, whereas genetic variation within the Eastern

Cluster was predicted by the composite model. Color morph frequency was not associated with genetic differentiation in *P. cinereus*. Using RD, waterways were the best predictor of morph frequency variation (Table 3a–b), while LCP found that geographic distance is the best predictor of morph frequency (Table 3c–d).

Correlates of genetic distance

In our study, elevation was the best predictor of genetic differentiation within the Central Cluster. In northern Ohio, elevation and topographic diversity increase from west to east (Fig. 2, Table 1, 2). Elevation has been shown to influence gene flow in other amphibians as well (Funk et al. 2005, Lowe et al. 2006, Giordano et al. 2007). For example, Takahashi and Pauley (2010) found *P. cinereus* reach different adult body sizes and differentially allocate resources at low versus high elevation, suggesting elevation influences local adaptation, which may impact genetic divergence. We expected environmental variables, rather than elevation, to correlate more strongly with genetic variation in *P. cinereus*, but our ENM may not have captured the fine-scale ecological features that affect niche use in plethodontid salamanders (Farallo and Miles 2016).

Isolation by environment, where genetic distance is correlated with environmental variation, affects patterns of population structure in a wide variety of organisms (Wang and Summers 2010, Shafer and Wolf 2013, Wang and Bradburd 2014), and a recent review by Sexton et al. (2014) found that in animals isolation by environment more commonly explains patterns of genetic variation than isolation by distance. Plethodontid salamanders lack lungs and depend on cutaneous respiration, and thus their dispersal behavior is heavily dependent upon cool, moist conditions (Spotila 1972, Feder 1983). For example, Peterman et al. (2014) found inferred rates of water loss best described genetic differences between populations in the western slimy salamander, *P. albagula*. While many factors influence population connectivity in *P. cinereus*, the salient result of our study is that all models found landscape resistance better represented patterns of genetic distance than geographic distance alone (Table 1, 2).

Correlates of morph frequency variation

Using RD, waterways had the greatest effect on morph frequency variation across all localities and within the Central Cluster (Fig. 1a, 2, Table 3a–b). Waterways have not been previously shown to affect variation in color morph frequency, but *P. cinereus* is a fully-terrestrial salamander that does not survive long when submerged in water, and thus waterways are likely important barriers. With LCP, we found that geographic distance was the most important factor influencing morph frequency variation. Across the entire range of *P. cinereus*, as well as within Ohio, the distribution of the striped/unstriped polymorphism fits a mosaic pattern (Anthony and Pfingsten 2013, Moore and Ouellet 2015), while in northern Ohio the striped/unstriped polymorphism appears to form a cline (Fig. 1a). Such a pattern is suggestive of secondary contact followed by lineage merger, or perhaps divergent selection between terminal portions of the range coupled with gene flow (McLean and Stuart-Fox 2014). However, we instead found three discrete genetic clusters with limited or no merger where they meet: the Eastern Cluster is fixed for the striped morph, while the Central Cluster is highly polymorphic; and the Western Cluster is nearly fixed for the unstriped morph. Thus, the broad clinal pattern in morph frequency across northern Ohio is not likely due to lineage merger or gene flow, but rather is the outcome of morph frequency variation in three genetic clusters.

Our discovery of three genetic clusters using microsatellites contrasts with a previous investigation of mtDNA variation by Radomski (2017). In that study, only two mtDNA clades were found in northern Ohio, and they form a secondary contact in the middle of our Central Cluster (Fig. 3). Discordance between mtDNA and nuclear markers is common and can have multiple causes (Toews and Brelsford 2012). One possibility is that the two mtDNA clades correspond with our Eastern and Central genetic clusters, but mitochondrial introgression has shifted the mtDNA boundary westward (Fig. 3). Alternatively, male-biased dispersal could be the cause of discordance (Prugnolle and de Meeus 2002), as males disperse over twice as far as females in *P. cinereus* (Liebgold et al. 2011). Under this scenario, the mtDNA contact zone could be located near the original point of secondary contact, while the nuclear genome contact zone has shifted over time. More work is needed to distinguish between the competing explanations for cyto-nuclear discordance.

It is also possible that morph frequency variation is associated with environmental or genetic factors on a finer-scale than measured in this study. For instance, several studies have found the unstriped morph of *P. cinereus* is associated with warmer temperatures, while the striped morph is more associated with cooler temperatures (reviewed by Cosentino et al. 2017). Similarly, a study by Fisher-Reid et al. (2013) on Long Island, New York found that a parapatrically distributed population of striped and unstriped morphs was correlated with microclimatic preferences. Dispersal behavior may also impact morph frequencies. Grant and Liebgold (2017) documented morph-biased dispersal in *P. cinereus* and found that unstriped morphs dispersed farther than striped morphs. The authors postulated that unequal dispersal may lead to variation in morph frequency across the range of *P. cinereus*. Additional studies within a geographic context may help elucidate patterns of morph frequency variation in *P. cinereus*.

Maintenance of the color polymorphism

The correlation of color morph frequency with waterways and geographic distance, coupled with discordance between morph frequency and genetic distance, suggests that gene flow alone is not maintaining the polymorphism. If gene

flow alone were maintaining the polymorphism, we would expect a correlation between morph frequency and genetic differentiation and higher rates of gene flow between populations with similar frequencies. Within the Central Cluster, low to moderate levels of gene flow and low levels of genetic drift suggest that these evolutionary forces do not strongly influence morph frequency variation among sites. An exception to this generalization can be found in sites 3 and 4, which are relatively isolated sites within the Central Cluster; these sites have a relatively high frequency of the unstriped morph and were more influenced by genetic drift than other populations (Supplementary material Appendix 1 Fig. A8). Among genetic clusters, genetic drift appears to have played a larger role in divergence, perhaps in part due to the Cuyahoga River acting as a barrier to gene flow between the Central and Eastern Clusters, and in part due to the isolation of the Western Cluster sites, which historically were separated from Central Cluster sites by the Great Black Swamp (Kaaz 1955; Fig. 1, Supplementary material Appendix 1 Fig. A6).

Our results suggest that the maintenance of the striped/unstriped polymorphism is not heavily dependent on any one evolutionary process, but instead relies upon a balance between gene flow, genetic drift and selection. This mix of evolutionary processes has been shown to influence color morph variation in other systems as well (Gray and McKinnon 2007, Antoniazza et al. 2010, Muñoz et al. 2013). For instance, a balance between natural selection, gene flow, and genetic drift maintain the banded/unbanded color pattern polymorphism in the Lake Erie water snake *Nerodia sipedon* (King and Lawson 1995). Our understanding of how selection operates on the morphs of *P. cinereus* remains unclear; however, selection appears to be an important mechanism as geographic distance, gene flow, and genetic drift alone do not explain patterns of morph frequency variation across our study sites. Possible selective processes include variation in selection across space and time, negative frequency-dependent selection, and niche partitioning within populations. Within the geographic range of the current study, Hantak and Kuchta (2018) found that the striped morph of *P. cinereus* was better camouflaged than the unstriped morph across multiple localities and seasons. If camouflage were the only trait under selection the polymorphism would not be maintained, suggesting other factors are at play. In another study, Fitzpatrick et al. (2009) used clay model replicas of the morphs to demonstrate that rare morphs have a survivorship advantage, suggesting negative frequency-dependent selection plays a role in the maintenance of the polymorphism. However, Kraemer et al. (2016) did not find evidence of negative frequency-dependent selection with mammalian predators. In addition, Grant et al. (2018) found no evidence of negative frequency-dependent selection in one population, although avian predation rates were higher and overall survivorship was lower in the striped morph. Finally, it is unclear how ecological niche divergence impacts color morph variation within and among populations.

In summary, using nuclear genetic markers we recovered three distinct genetic clusters in northern Ohio. Isolating barriers, such as inhospitable terrain and environmental conditions, appear to have promoted divergence, followed by the compounding consequence of increased genetic drift through a lack of gene flow. Past studies on the maintenance of the polymorphism in *P. cinereus* have produced a diversity of findings. Here, we found that waterway barriers and geographic distance, coupled with genetic drift, are correlated with divergence in morph frequency, while gene flow counteracts divergence. The mechanisms promoting variation in morph frequency among populations within the Central Cluster remain unclear, and it may be that there is geographic variation in the evolutionary mechanisms maintaining the polymorphism. Overall, our study suggests that a mix of gene flow, genetic drift, and selection interact to maintain the enigmatic striped/unstriped polymorphism.

Acknowledgements – We thank Kyle Brooks and Olivia Brooks for assistance with sample collection, and Garrett Sisson and Alex Cameron for GIS advice. We also thank Bill Peterman for assistance with ResistanceGA. Kyle Brooks provided photos of the *P. cinereus* morphs.

Funding – Financial support was provided to MMH by the Society for the Study of Evolution Rosemary Grant Award and the Ohio University Student Enhancement Award.

Author contributions – MMH and SRK designed the study. MMH, SRK, CDA and CAMH collected samples. MMH, RBP and PEC conducted laboratory work and analyzed data. MMH and SRK wrote the manuscript. All authors contributed to draft and final versions of the manuscript.

Permits – Salamander tissue was collected with an Ohio Department of Natural Resources Permit (17-19) to MMH, and data collection was approved by the Ohio University Institutional Animal Care and Use Committee (12-L-050).

References

Acord, M. A. et al. 2013. Assortative mating in a polymorphic salamander. – Copeia 2013: 676–683.

Adriaensen, F. et al. 2003. The application of 'least-cost' modeling as a functional landscape model. – Landscape Urban Plan. 64: 233–247.

Allen, J. A. 1988. Frequency-dependent selection by predators [and Discussion]. – Phil. Trans. R. Soc. B 319: 485–503.

Anthony, C. D. and Pfingsten, R. A. 2013. Eastern red-backed salamander. *Plethodon cinereus* (Green 1818). – In: Pfingsten, R. A. et al. (eds), Amphibians of Ohio. – Ohio Biological Survey, pp. 335–360.

Anthony, C. D. et al. 2008. Ecological separation in a polymorphic terrestrial salamander. – J. Anim. Ecol. 77: 646–653.

Anthony, C. D. et al. 2017. Differences in prey availability within the territories of striped and unstriped eastern red-backed salamanders (*Plethodon cinereus*). – Herpetol. Rev. 48: 509–514.

Antoniazza, S. et al. 2010. Local adaptation maintains clinal variation in melanin-based coloration of European barn owls (*Tyto alba*). – Evolution 85: 797–807.
Avon, C. and Bergès, L. 2016. Prioritization of habitat patches for landscape connectivity conservation differs between least-cost and resistance distances. – Landscape Ecol. 31: 1551–1565.
Beerli, P. 2008. Migrate ver. 3.6.5: a maximum likelihood and Bayesian estimator of gene flow using the coalescent. – <http://popgen.scs.edu/migrate.html>.
Beerli, P. and Palczewski, M. 2010. Unified framework to evaluate panmixia and migration direction among multiple sampling locations. – Genetics 185: 313–326.
Burton, T. M. and Likens, G. E. 1975 Salamander populations and biomass in the Hubbard Brook experimental forest, New Hampshire. – Copeia 1975: 541–546.
Cabe, P. R. et al. 2007. Fine-scale population differentiation and gene flow in a terrestrial salamander (*Plethodon cinereus*) living in continuous habitat. – Heredity 98: 53–60.
Cain, A. J. and Sheppard, P. M. 1954 Natural selection in Cepaea. – Genetics 89–116.
Cameron, A. C. et al. 2017. Assessment of intra and interregional genetic variation in the eastern red-backed salamander, *Plethodon cinereus*, via analysis of novel microsatellite markers. – PLoS One 12: e0186866.
Chapuis, M.-P. and Estoup, A. 2007. Microsatellite null alleles and estimation of population differentiation. – Mol. Biol. Evol. 24: 621–631.
Clarke, R. T. et al. 2002. Confidence limits for regression relationships between distance matrices: estimating gene flow with distance. – J. Agric. Biol. Environ. Stat. 7: 361–372.
Converse, P. E. et al. 2015. Spatiotemporal analysis of gene flow in Chesapeake Bay diamondback terrapins (*Malaclemys terrapin*). – Mol. Ecol. 24: 5864–5876.
Corl, A. et al. 2010. Selective loss of polymorphic mating types is associated with rapid phenotypic evolution during morphic speciation. – Proc. Natl Acad. Sci. USA 107: 4254–4259.
Cosentino, B. J. et al. 2017. Evolutionary response to global change: climate and land use interact to shape color polymorphism in a woodland salamander. – Ecol. Evol. 7: 5426–5434.
Davis Rabosky, A. R. et al. 2016. Unlinked Mendelian inheritance of red and black pigmentation in snakes: implications for Batesian mimicry. – Evolution 70: 944–953.
Earl, D. A. and vonHoldt, B. M. 2012. Structure Harvester: a website and program for visualizing structure output and implementing the Evanno method. – Conserv. Genet. Resour. 4: 359–361.
Endler, J. A. 1978. A predator's view of animal color patterns. – Evol. Biol. 11: 319–364.
Evanno, G. et al. 2005. Detecting the number of clusters of individuals using the software STRUCTURE: a simulation study. – Mol. Ecol. 14: 2611–2620.
Farallo, V. R. and Miles, D. B. 2016. The importance of microhabitat: a comparison of two microendemic species of *Plethodon* to the widespread *P. cinereus*. – Copeia 104: 67–77.
Feder, M. E. 1983. Integrating the ecology and physiology of plethodontid salamanders. – Herpetologica 39: 291–310.
Fisher-Reid, M. C. et al. 2013. Parapatric divergence of sympatric morphs in a salamander: incipient speciation on Long Island? – Mol. Ecol. 22: 4681–4694.
Fitzpatrick, B. M. et al. 2009. Frequency-dependent selection by wild birds promotes polymorphism in model salamanders. – BMC Ecol. 9: 12.
Ford, E. B. 1945. Polymorphism. – Biol. Rev. 73–88.
Forsman, A. et al. 2008. A model of ecological and evolutionary consequences of color polymorphism. – Ecology 89: 34–40.
Funk, W. C. et al. 2005. Population structure of Columbia spotted frogs (*Rana luteiventris*) is strongly affected by the landscape. – Mol. Ecol. 14: 483–496.
Funk, W. C. et al. 2009. Genetic divergence is more tightly related to call variation than landscape features in the Amazonian frogs *Physalaemus petersi* and *P. freibergi*. – J. Evol. Biol. 22: 1839–1853.
Giordano, A. R. et al. 2007. The influence of altitude and topography on genetic structure in the long-toed salamander (*Ambystoma macrodactulym*). – Mol. Ecol. 16: 1625–1637.
Grant, A. H. and Liebgold, E. B. 2017. Color-biased dispersal inferred by fine-scale genetic spatial autocorrelation in a color polymorphic salamander. – J. Hered. 108: 588–593.
Grant, A. H. et al. 2018. Differential survival and the effects of predation on a color polymorphic species, the red-backed salamander (*Plethodon cinereus*). – J. Herpetol. 52: 127–135.
Gray, S. M. and McKinnon, J. S. 2007. Linking color polymorphism maintenance and speciation. – Trends Ecol. Evol. 22: 71–79.
Hantak, M. M. and Kuchta, S. R. 2018. Predator perception across space and time: relative camouflage in a colour polymorphic salamander. – Biol. J. Linn. Soc. 123: 21–33.
Hantak, M. M. et al. 2016. Comparison of the diets of sympatric erythristic and striped morphs of *Plethodon cinereus* (eastern red-backed salamander). – Northeast. Nat. 23: 219–228.
Hantak, M. M. et al. 2019. Data from: do genetic structure and landscape heterogeneity impact color morph frequency in a polymorphic salamander? – Dryad Digital Repository, <http://dx.doi.org/10.5061/dryad.j807218>.
Highton, R. 1962. Revision of North American salamanders of the genus *Plethodon*. – Bull. Florida State Mus. 6: 236–367.
Highton, R. 2004. A new species of woodland salamander of the *Plethodon cinereus* group from the Blue Ridge Mountains of Virginia. – Jeffersoniana 14: 1–22.
Hijmans, R. J. et al. 2005. Very high resolution interpolated climate surfaces for global land areas. – Int. J. Climatol. 25: 1965–1978.
Jakobsson, M. and Rosenberg, N. A. 2007. CLUMPP: a cluster matching and permutation program for dealing with label switching and multimodality in analysis of population structure. – Bioinformatics 23: 1801–1806.
Janes, J. K. et al. 2017. The K = 2 conundrum. – Mol. Ecol. 26: 3594–3602.
Jombart, T. 2008. adegenet: a R package for the multivariate analysis of genetic markers. – Bioinformatics 24: 1403–1405.
Jombart, T. et al. 2010. Discriminant analysis of principal components: a new method for the analysis of genetically structured populations. – BMC Genet. 11: 94.
Jost, L. 2008. GST and its relatives do not measure differentiation. – Mol. Ecol. 17: 4015–4026.
Kaaz, M. R. 1955. The Black Swamp: a study in historical geography. – Ann. Assoc. Am. Geogr. 35: 1–35.
Kalinowski, S. T. 2005. HP-RARE 1.0: a computer program for performing rarefaction on measures of allelic richness. – Mol. Ecol. Notes 5: 187–189.
Karhunen, M. and Ovaskainen, O. 2012. Estimating population-level coancestry coefficients by an admixture F model. – Genetics 192: 609–617.
Kearse, M. et al. 2012. Geneious basic: an integrated and extendable desktop software platform for the organization and analysis of sequence data. – Bioinformatics 28: 1647–1649.

King, R. B. and Lawson, R. 1995. Color-pattern variation in Lake Erie water snakes: the role of gene flow. – Evolution 49: 885–896.
Kraemer, A. C. et al. 2016. Both novelty and conspicuousness influence selection by mammalian predators on the colour pattern of *Plethodon cinereus* (Urodela: Plethodontidae). – Biol. J. Linn. Soc. 118: 889–900.
Liebgold, E. B. et al. 2011. Female philopatry and male-biased dispersal in a direct-developing salamander, *Plethodon cinereus*. – Mol. Ecol. 20: 249–257.
Lowe, W. H. et al. 2006. Linking direct and indirect data on dispersal: isolation by slope in a headwater stream salamander. – Ecology 87: 334–339.
Manel, S. and Holderegger, R. 2013. Ten years of landscape genetics. – Trends Ecol. Evol. 28: 614–621.
Manel, S. et al. 2003. Landscape genetics: combining landscape ecology and population genetics. – Trends Ecol. Evol. 18: 189–197.
Marrotte, R. R. and Bowman, J. 2017. The relationship between least-cost and resistance distance. – PLoS One 12: e0174212.
Mazerolle, M. J. 2013. Package 'AICcmodavg'. – The R Project for Statistical Computing, Vienna, Austria.
Meirmans, P. G. and van Tienderen, P. H. 2004. Genotype and Genodive: two programs for the analysis of genetic diversity of asexual organisms. – Mol. Ecol. Notes 4: 792–794.
McClure, M. L. et al. 2016. Connecting models to movements: testing connectivity model predictions against empirical migration and dispersal data. – Landsc. Ecol. 31: 1419–1432.
McLean, C. A. and Stuart-Fox, D. 2014. Geographic variation in animal colour polymorphisms and its role in speciation. – Biol. Rev. 89: 860–873.
McLean, C. A. et al. 2015. Environment, but not genetic divergence, influences geographic variation in colour morph frequencies in a lizard. – BMC Evol. Biol. 15: 156.
McRae, B. 2006. Isolation by resistance. – Evolution 60: 1551–1561.
Moore, J.-D. and Ouellet, M. 2015. Questioning the use of an amphibian colour morph as an indicator of climate change. – Global Change Biol. 21: 566–571.
Muñoz, M. M. et al. 2013. Divergence in coloration and ecological speciation in the *Anolis marmoratus* species complex. – Mol. Ecol. 22: 2668–2682.
Paluh, D. J. et al. 2015. Selective foraging on ants by a terrestrial polymorphic salamander. – Am. Midl. Nat. 174: 265–277.
Peakall, R. and Smouse, P. E. 2012. GenAlEx 6.5: genetic analysis in Excel. Population genetic software for teaching and research – an update. – Bioinformatics 28: 2537–2539.
Peterman, W. E. 2018. ResistanceGA: an Rpackage for the optimization of resistance surfaces using genetic algorithms. – Methods Ecol. Evol. 49: 340–10.
Peterman, W. E. and Semlitsch, R. D. 2013. Fine-scale habitat associations of a terrestrial Salamander: the role of environmental gradients and implications for population dynamics. – PLoS One 8: e62184.
Peterman, W. E. et al. 2014. Ecological resistance surfaces predict fine-scale genetic differentiation in a terrestrial woodland salamander. – Mol. Ecol. 23: 2402–2413.
Phillips, S. J. et al. 2006. Maximum entropy modeling of species geographic distributions. – Ecol. Model. 190: 231–259.
Pritchard, J. K. et al. 2000. Inference of population structure using multilocus genotype data. – Genetics 155: 945–959.
Prugnolle, F. and de Meeus, T. 2002. Inferring sex-biased dispersal from population genetic tools: a review. – Heredity 88: 161–165.
Radomski, T. P. 2017. Biogeography and climatic niche evolution in the eastern red-backed salamander. – MS thesis, Ohio Univ., USA.
Reiter, M. K. et al. 2014. Territorial behavior and ecological divergence in a polymorphic salamander. – Copeia 2014: 481–488.
Rosenberg, N. A. 2004. Distruct: a program for the graphical display of population structure. – Mol. Ecol. Notes 4: 137–138.
Rousset, F. 2008. Genepop'007: a complete re-implementation of the genepop software for Windows and Linux. – Mol. Ecol. Resour. 8: 103–106.
Sandoval, C. P. 1994. The effects of the relative geographic scales of gene flow and selection on morph frequencies in the walking-stick *Timema cristinae*. – Evolution 48: 1866–1879.
Scrucca, L. 2013. GA: a package for genetic algorithms in R. – J. Stat. Softw. 53: 1–37.
Sexton, J. P. et al. 2014. Genetic isolation by environment or distance: which pattern of gene flow is most common? – Evolution 68: 1–15.
Shafer, A. B. A. and Wolf, J. B. W. 2013. Widespread evidence for incipient ecological speciation: a meta-analysis of isolation-by-ecology. – Ecol. Lett. 16: 940–950.
Sinervo, B. and Lively, C. M. 1996. The rock-paper-scissors game and the evolution of alternative male strategies. – Nature 380: 240–243.
Sinervo, B. and Svensson, E. 2002. Correlational selection and the evolution of genomic architecture. – Heredity 89: 329–338.
Slatkin, M. 1987. Gene flow and the geographic structure of natural populations. – Science 236: 787–792.
Spear, S. F. et al. 2005. Landscape genetics of the blotched tiger salamander (*Ambystoma tigrinum melanostictum*). – Mol. Ecol. 14: 2553–2564.
Spotila, J. R. 1972. Role of temperature and water in the ecology of lungless salamanders. – Ecol. Monogr. 42: 95–125.
Storfer, A. et al. 2007. Putting the 'landscape' in landscape genetics. – Heredity 98: 128–142.
Storfer, A. et al. 2010. Landscape genetics: where are we now? – Mol. Ecol. 19: 3496–3514.
Stuczka, A. et al. 2016. Niche partitioning along the diet axis in a colour polymorphic population of eastern red-backed salamanders, *Plethodon cinereus*. – Amphibia-Reptilia 37: 283–290.
Svensson, E. et al. 2001. Density-dependent competition and selection on immune function in genetic lizard morphs. – Proc. Natl Acad. Sci. USA 98: 12561–12565.
Takahashi, M. K. and Pauley, T. K. 2010. Resource allocation and life history traits of *Plethodon cinereus* at different elevations. – Am. Midl. Nat. 163: 87–94.
Toews, D. P. and Brelsford, A. 2012. The biogeography of mitochondrial and nuclear discordance in animals. – Mol. Ecol. 21: 3907–3930.
van Etten, J. 2017. R package gdistance: distances and routes on geographical grids. – J. Stat. Softw. 76: 1–21.

van Oosterhout, C. et al. 2004. micro-checker: software for identifying and correcting genotyping errors in microsatellite data. – Mol. Ecol. Notes 4: 535–538.
van Strien, M. J. et al. 2012. A new analytical approach to landscape genetic modelling: least-cost transect analysis and linear mixed models. – Mol. Ecol. 21: 4010–4023.
Wang, I. J. 2009. Fine-scale population structure in a desert amphibian: landscape genetics of the black toad (*Bufo exsul*). – Mol. Ecol. 18: 3847–3856.

Supplementary material (available online as Appendix ecog-04534 at <www.ecography.org/appendix/ecog-04534>). Appendix 1.

Wang, I. J. and Bradburd, G. S. 2014. Isolation by environment. – Mol. Ecol. 23: 5649–5662.
Wang, I. J. and Summers, K. 2010. Genetic structure is correlated with phenotypic divergence rather than geographic isolation in the highly polymorphic strawberry poison-dart frog. – Mol. Ecol. 19: 447–458.
West-Eberhard, M. J. 1986. Alternative adaptations, speciation and phylogeny (a review). – Proc. Natl Acad. Sci. USA 83: 1388–1392.